Concept Vehicles for VTOL Air Taxi Operations

Wayne Johnson **Christopher Silva** **Eduardo Solis**
NASA Ames Research Center Science & Technology Corp.
Moffett Field, California Moffett Field, California
wayne.johnson@nasa.gov christopher.silva@nasa.gov eduardo.solis@nasa.gov

ABSTRACT

Concept vehicles are presented for air taxi operations, also known as urban air mobility or on-demand mobility applications. Considering the design-space dimensions of payload (passengers and pilot), range, aircraft type, and propulsion system, three aircraft are designed: a single-passenger (250-lb payload), 50-nm range quadrotor with electric propulsion; a six-passenger (1200-lb payload), 4x50 = 200-nm range side-by-side helicopter with hybrid propulsion; and a fifteen-passenger (3000-lb payload), 8x50 = 400-nm range tiltwing with turbo-electric propulsion. These concept vehicles are intended to focus and guide NASA research activities in support of aircraft development for emerging aviation markets, in particular VTOL air taxi operations. Research areas are discussed, illustrated by results from the design of the concept vehicles.

INTRODUCTION[·]

Urban air taxi operations, also known as urban air mobility or on-demand mobility applications, are enabled by vertical take-off and landing (VTOL) capability, power and energy requirements are minimized by using low disk-loading rotors, and short range requirements permit consideration of non-traditional propulsion concepts. The community of innovation has recognized that technology advances in structures, automation and control, energy generation-storage-utilization, and tools for design and analysis, coupled with pressures of resource availability and population density, make this the right time to explore new ways to move people and goods (ref. 1). The objective of the present work is to identify concept vehicles that can be used to focus and guide NASA research activities in support of aircraft development for emerging aviation markets, in particular VTOL air taxi operations.

To meet this objective, the designs are carried far enough to identify crucial technologies and research requirements, to explore a range of aircraft types, propulsion system types, and size, and to examine sensitivities to trades of requirements. While identifying relevant issues and major technical deficiencies is important, resolving all questions is not necessary, and component weight estimates and performance models can be the subject of future work. With this approach, the specific design choices made are not important, as long as primary and relevant research requirements are covered. Indeed, to these ends it is best that NASA concept vehicles be different in appearance and design detail from prominent industry arrangements.

The air taxi design community is considering a wide range of aircraft attributes:

a) number of passengers (including pilot): 1, 2, 4, 6, 15, 30;
b) un-refueled range: 50, 100, 200, 400, 800 nm (here as multiples of 50 nm segments);
c) market: air taxis, commuter scheduled, mass transit, airline;
d) aircraft type: multicopter, side-by-side, tiltwing, tiltrotor, lift+cruise, vectored thrust, compound, helicopter;
e) propulsion system: turboshaft, turboelectric, electric, parallel hybrid, fuel cell, diesel.

Three concept vehicles are developed that span many elements of this design space:

[·]*Presented at the AHS Technical Conference on Aeromechanics Design for Transformative Vertical Flight, San Francisco, CA, January 16-19, 2018.*

1) A single-passenger (250-lb payload), 50-nm range quadrotor with electric propulsion (figure 1), using flapping rotors and collective control; design excursions include rigid rotors, rotor speed control, and reciprocating engines.

2) A six-passenger (1200-lb payload), 4x50 = 200-nm range side-by-side helicopter with hybrid propulsion (figure 2).

3) A fifteen-passenger (3000-lb payload), 8x50 = 400-nm range tiltwing with turbo-electric propulsion (figure 3), using four propellers with collective and cyclic control; design excursions include tail propellers for pitch and directional control.

Based on these aircraft (and numerous excursions), the research requirements for air taxi aircraft development (figure 4) include propulsion system efficiency; performance; rotor-rotor interactions, rotor-wing interactions, aircraft design, structure and aeroelasticity, noise and annoyance, operational effectiveness, and safety and airworthiness.

Figure 1. Single-passenger quadrotor with electric propulsion.

Figure 2. Six-passenger side-by-side helicopter with hybrid propulsion.

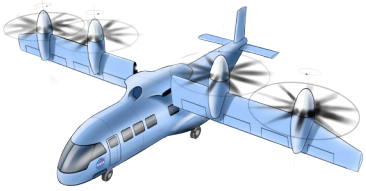

Figure 3. Fifteen-passenger tiltwing with turboelectric propulsion.

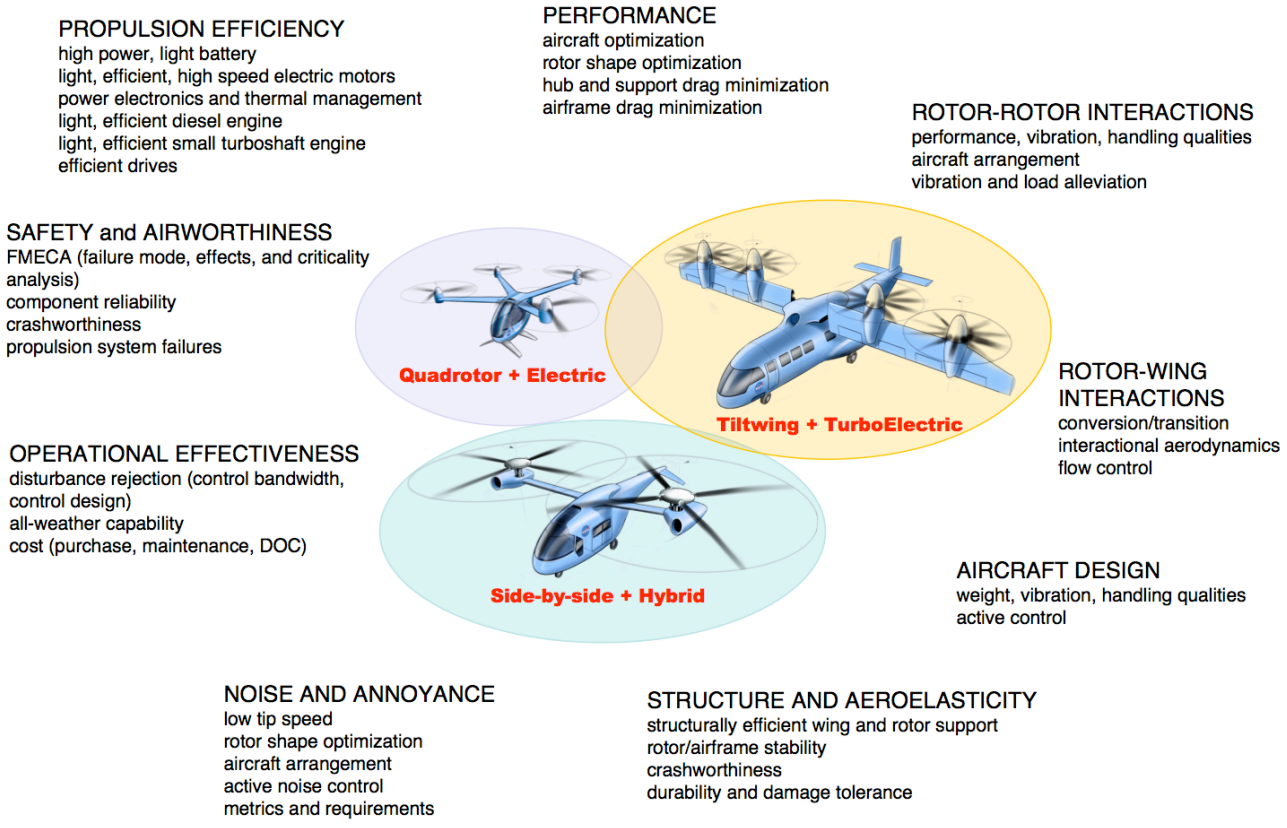

Figure 4. Research areas for air taxi aircraft development.

DESIGN AND ANALYSIS TOOLS

The aircraft were sized and optimized using NDARC, considering the aircraft type, propulsion system, and rotor parameters. Performance was optimized using the rotorcraft comprehensive analysis CAMRAD II.

Rotorcraft Sizing and Analysis NDARC

The concept vehicles were sized using NDARC (NASA Design and Analysis of Rotorcraft), which is a conceptual/preliminary design and analysis code for rapidly sizing and conducting performance analysis of new aircraft concepts (refs. 2–4). NDARC has a modular architecture, facilitating its extension to new aircraft and propulsion types, including non-traditional propulsion systems (ref 5). The design task sizes the vehicle to satisfy a set of design conditions and missions. The aircraft size is characterized by parameters such as design gross weight, weight empty, component dimensions, drive system torque limit, fuel tank capacity, and engine power. The analysis tasks include off-design mission analysis and flight performance calculation for point operating conditions. To achieve flexibility in configuration modeling, NDARC constructs a vehicle from a set of components, including fuselage, rotors, wings, tails, transmissions, and engines. For efficient program execution, each component uses surrogate models for performance and weight estimation. Higher fidelity component design and analysis tools as well as databases of existing components provide the information needed to calibrate these surrogate models, including the influence of size and technology level. The reliability of the synthesis and evaluation results depends on the accuracy of the calibrated component models. Reference 4 illustrates the calibration and validation process for NDARC.

Comprehensive Analysis CAMRAD II

Performance analyses were conducted with the comprehensive rotorcraft analysis CAMRAD II (refs. 6–8). CAMRAD II is an aeromechanics analysis of rotorcraft that incorporates a combination of advanced technologies, including multibody dynamics, nonlinear finite elements, and rotorcraft aerodynamics. The trim task finds the equilibrium solution for a steady state operating condition, and produces the solution for performance, loads, and vibration. The CAMRAD II aerodynamic model for the rotor blade is based on lifting-line theory, using steady two-dimensional airfoil characteristics and a vortex wake model. CAMRAD II has undergone extensive correlation with performance and loads measurements on rotorcraft.

Performance calculations for calibration of the NDARC rotor models considered first an isolated rotor, in particular to define profile power including the influence of stall. Then calculations for the multi-rotor system were used to calibrate the rotor-rotor interference effects on induced and profile power.

DESIGN REQUIREMENTS

General Design Missions and Conditions

The primary sizing mission, summarized in table 1, consists of the following segments: (1) 2 min hover out-of-ground-effect (OGE) for takeoff; (2) fly 50 nm at best-range speed; (3) 2 min hover OGE for landing; (4) fuel/energy reserve minimum of 10% of mission or 20 min flight at best-endurance speed. All the segments are flown at atmospheric conditions of 5000-ft altitude and ISA+20°C temperature. Segments 1–3 are repeated for each 50 nm leg in the un-refueled range. Cruise is flown at best-range speed (99% high side), unless the maximum speed is less than V_{br}. Reserve requirements are based on 14 CFR 91.151: 20 min at cruise speed for VFR rotorcraft. A second sizing mission has these segments flown at sea level and ISA+20°C temperature.

All weather operations are assumed, which has an impact on systems weight (including de-icing). For low aircraft noise, the design rotor tip speed is low: 450 ft/sec for the quadrotor, 550 ft/sec for the larger aircraft. Maximum speed (from power available at 90% MCP) is fallout, with installed power determined by takeoff conditions.

Approaches to deal with component failures in the propulsion system are needed, but the impact of such failures is only partially accounted for in these concept vehicle designs. For conventional propulsion systems, identifying approaches for safe one-engine inoperative (OEI) flight, including takeoff operations and power requirements, and the requirements for all-engine inoperative (AEI) operations and/or autorotation capability is needed. Similar requirements must be developed for the non-traditional propulsion systems.

The two sizing missions determine design gross weight (DGW), fuel tank capacity, installed power, and transmission limits. A sizing condition at DGW, 5k/ISA+20°C, and 95% MRP determines the maximum takeoff weight.

Missions for Specific Aircraft Types

For the hybrid propulsion system, the motor/generator size is fixed (100 hp IRP for the six-passenger aircraft).

Missions start with the battery fully charged. For hover segments and conditions, the motor operates at 100% IRP. For cruise segments, the generator charges the battery at 10% MCP. For the reserve segment, the generator is off. The battery is sized by a mission (table 1) of 10 min hover, equivalent to 5 takeoffs or landings without recharging.

For the turboelectric propulsion system, the battery is sized by a mission (table 1) of 2 min hover OGE with the turboshaft or generator out — corresponding to a discharge rate of C=30 1/hr, which no doubt would require battery replacement. In normal operation, the generator power is adjusted so generator energy flow equals the total motor energy flow (trim to zero net energy through the battery).

The tiltwing aircraft has two gear states (hover at 100% rpm, cruise at 50% rpm, with gear shift between motor and propeller) and two control states (helicopter mode rotor controls, airplane mode wing/tail controls). In conversion, the aircraft is trimmed using rotor collective and wing flap, at fixed aircraft pitch angle.

Table 1. Aircraft sizing missions.

Primary mission						
segment		atmosphere	time	distance	speed	engine
1	hover	5k/ISA+20°C	2		0	≤ 95% IRP
2	cruise	5k/ISA+20°C		50 nm	V_{br}*	≤ 100% MCP
3	hover	5k/ISA+20°C	2		0	≤ 95% IRP
4	20 min / 10% reserve	5k/ISA+20°C	20		V_{be}	≤ 100% MCP
segments 1–3 repeated for each 50 nm leg						
Secondary mission						
		SL/ISA+20°C				
Hybrid battery charging						
segment		atmosphere	time	distance	speed	motor
1	hover DGW	5k/ISA+20°C	10		0	100% IRP
Turboelectric battery sizing						
segment		atmosphere	time	distance	speed	motor
1	hover DGW	5k/ISA+20°C	2		0	≤ 100% IRP

*$V_{cruise} = V_{br}$ if $V_{br} < V_{max}$; V_{cruise} = 70 knots for single-passenger quadrotor

TECHNOLOGY

Battery

Light and efficient batteries are crucial to producing good designs for electric aircraft. The battery technology considered is summarized in table 2. The baseline designs use an installed battery specific energy of 400 Wh/kg. Typical Li-ion battery discharge characteristics (figure 5) are used to calculate the battery efficiency. The internal resistance reduces efficiency at high discharge rates. Margins for maximum charge and discharge are established to prolong battery life (in terms of discharge-charge cycles): charge to within 5–10% of full capacity (depth-of-discharge 0.05–0.10), discharge to 15–20% capacity (depth-of-discharge 0.80–0.85). Current delivery limits for cells are specified as a C-rate (capacity/hr). The convention for the present designs is that the battery capacity refers to the usable energy, with the pack specific energy accounting for minimum and maximum depth-of-discharge limits. (Alternatively, the battery capacity could be increased above mission requirements to account for unusable energy, and the missions started at less than full capacity to reflect charge limitations.) Even with a high maximum burst discharge capability (maximum power), discharge currents must be limited to 2–3C for good battery life. The installed specific energy is reduced by packaging and conditioning requirements, including thermal management systems. Table 2 shows uninstalled (cell), useable, and installed (battery) specific energy in Wh/kg, for several technology levels. The battery technology level is here characterized by the installed specific energy.

Table 2. Battery technology.

technology		current				advanced
FuelTank	units					
uninstalled specific energy	Wh/kg	240	300	325	487.5	650
usable energy fraction		70%	75%	80%	80%	80%
usable specific energy	Wh/kg	168	225	260	390	530
energy density	MJ/L	1.3	1.5	1.6	2.05	2.25
installation fraction		0.8	0.5	0.3	0.3	0.3
installed specific energy	Wh/kg	93.33	150	200	300	400
BatteryModel						
max burst discharge	1/hr	4.	6.	8.	14.	20.
max charge	1/hr	1.	1.5	2.	3.	4.
depth of discharge min		0.10	0.05	0.05	0.05	0.05
depth of discharge max		0.80	0.80	0.85	0.85	0.85

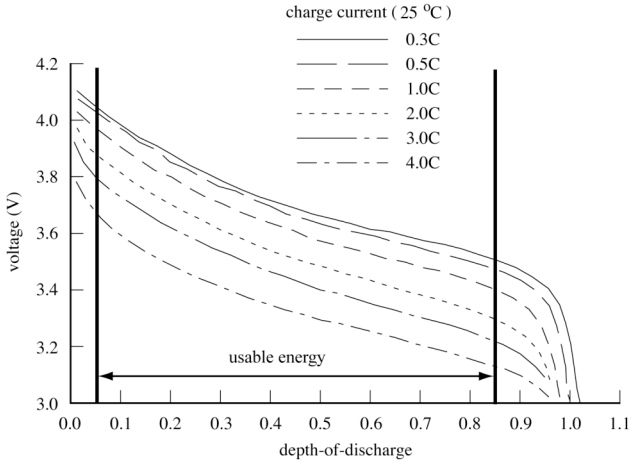

Figure 5. Typical Li-ion battery discharge characteristics.

Motors and Generators

All of the present designs use high-speed/low-torque motors and generators, hence have a transmission from the motor to low-speed/high-torque rotors. The motor weight estimate includes the speed controller, inverter, and thermal management (coolant, ducting, radiator, etc.). The NDARC parametric motor weight model (ref. 2) is

$$W = 0.5382 Q^{0.8129}$$

for weight in lb, and peak torque Q in ft-lb. This regression equation is based on 64 motors, from 20–550 hp, 100–10000 rpm, with average error of 25% for high torque-to-weight motors ($Q/W > 3.5$ ft-lb/lb, many of which are low rpm). As a good state-of-the-art motor, the Tesla model S motor (70 lb for performance mode power of 375 kW at 5950 rpm) gives a calibration factor of 0.9169. For advanced technology motors, it is assumed that these performance mode characteristics can be used for IRP (30 min) and MRP (10 min) ratings, with a design speed of 8000 rpm. Table 3 summarizes the assumptions for motor balance of plant. The motor efficiency is assumed to be constant, independent of torque and speed.

The motor/generator weight and performance are estimated as follows: NDARC high torque-to-weight weight regression, with technology factor 1.63 to account for the entire motor system weight; IRP = 150% MCP; reference rotational speed 8000 rpm; constant efficiency η = 95%. The resulting total weight efficiency is 0.38 lb/hp for the quadrotor (4x22 hp), 0.24 lb/hp for the side-by-side (2x216 hp), 0.20 lb/hp for the tiltwing motors (4x641 hp), and 0.15 lb/hp for the tiltwing generator (2840 hp).

Table 3. Motor/generator balance of plant.

	controller/ inverter	thermal management	technology factor
Small engine (20 hp)	60%	10%	1.614
Large engine (≥100 hp)	20%	50%	1.650

Propulsion System Modeling Assumptions

All transmissions modeled here have losses of 2%. Turboshaft and reciprocating engine fuel flow is increased as usual by 5% to account for engine degradation. Accessory losses are 5 hp for the single-passenger quadrotor, 20 hp for the six-passenger side-by-side, and 50 hp for the fifteen-passenger tiltwing.

Internal Combustion Engines

Turboshaft and reciprocating engine technology is specified by weight/power and specific fuel consumption (table 4). The tiltwing turboshaft engine model (nominally 750 hp) is based on the CTS800 (c.2000

technology) and Allison 250-C40B engines, scaled as for the generic 1000 hp engine model (ref. 2). The tiltwing turboelectric engine model (nominally 400 hp) is based on the AATE (TRL 6 in 2015). The side-by-side turboshaft engine is based on the RR300 (TRL 9 since early 2000s) and Allison 250/T63-A-5 (1970s technology) engines, scaled as for the generic 500 hp engine model. The quadrotor turboshaft engine model is an extrapolation to 100 hp. The quadrotor reciprocating engine model is based on the Rotax and Continental IO-550-B engines; gasoline density is 6.0 lb/gal. The quadrotor diesel engine model is based on the Continental/Technify Motors CD-155; diesel fuel density is 7.0 lb/gal.

Table 4. Turboshaft and reciprocating engines.

aircraft	engine	size hp	weight lb/hp	MCP SLS sfc lb/hp-hr
tiltwing	turboshaft	4000	0.14	0.35
tiltwing	turboshaft	750	0.23	0.48
side-by-side	turboshaft	200	0.50	0.54
quadrotor	turboshaft	100	0.70	0.70
quadrotor	recip	100	1.65	0.47
quadrotor	diesel	100	1.90	0.38

Weights

The design gross weight is the mission takeoff weight. The structural design gross weight is taken as the design gross weight, with an ultimate load factor of 4. The maximum takeoff weight is calculated for hover OGE, at 95% MRP.

NDARC parametric weight models (ref. 2) are used for fuselage, flight controls, landing gear, rotor hub and blades, gear box, drive shaft, wing, and propeller. The data base behind these models includes small aircraft and stiff rotors (table 5). The wing data base includes the tiltwing XC-142A (calibration factor 0.79). The propeller data base includes the tiltwings XC-142A (calibration factor 0.78) and CL-84 (calibration factor 0.94).

Traditional allocations are used for avionics equipment, for furnishings, and for environmental control. The technology factors reflect light-weight, rugged composite fuselage, light-weight composite rotor system, fuel efficient and light weight turboshaft engines, and weight efficient drive systems. Table 6 gives the tech factors used in the designs. For the quadrotor, rotor support weight of 2.0 lb/ft is used. The rotor support (wing) weight of the side-by-side aircraft is obtained using the tiltrotor weight model, for a 2.0g jump takeoff and a wing torsion frequency of 0.8/rev. The flight controls are electric, hence there is no hydraulic system weight. For the quadrotor with rotor speed control, there is no rotor control system weight, and a fuselage weight increment of 25 lb is included to cover the AEI design solution. System weights are summarized in table 7. Electrical system weight is 10 lb plus 10 lb/persion. Environmental system weight is 15 lb/person.

Table 5. Data base for NDARC rotor parametric weight model.

small aircraft	weight (lb)	radius (ft)
OH-6A	2700	13.17
OH-58C	3200	17.7
269B	896	12.6
stiff rotors	flap frequency (per-rev)	
BO-105	1.12	
AH-56A	1.12	
XV-15	1.25	
XH-59A	1.40	

Table 6. Technology factors for all designs (net, including calibration factors).

rotor flight control	
boosted controls	0.46 / 0.30 *
actuators	0.71 / 0.50 *
non-boosted controls	1.10 / 0.90 *
fuselage	
basic	0.76
crashworthiness	0.90
crash weight	15% / 6% / 6% basic **
landing gear	
basic	1.00
crash weight	15% basic
rotor	
blade	0.92
hub	0.76
propeller	
tiltwing	1.40
tiltwing tail	1.50
fuel tank	
tank	0.84
plumbing	0.66
drive system	
gear box	0.74
drive shaft	0.69
engine group	
cowling	0.50
pylon	0.85
support	1.10
accessories	0.82
wing	
side-by-side	0.80
tiltwing basic	0.65
fairing+fitting+flap	18% basic

* with cyclic / only collective

** quadrotor / side-by-side / tiltwing

Table 7. System weights (lb).

aircraft	quadrotor	side-by-side	tiltwing
number of passengers	1	6	15
passenger weight	250	200	200
trapped fluids	5	10	20
vibration weight, flapping rotor	3% WE	2% WE	
vibration weight, rigid rotor	5% WE		2% WE
contingency weight	5% WE	5% WE	5% WE
automatic flight control	40	40	40
instruments	10	10	10
mission equipment	40	40	40
electrical	20	70	160
environmental	15	90	225
furnishings	31	178	443

Drag

Table 8 summarizes the drag build up. For each aircraft, the fuselage geometry is fixed, with values for length, width, height, wetted area, and projected area obtained from OpenVSP models. It is assumed that each aircraft has a well-designed and built low-drag fuselage. Landing gear drag is D/q = 0.2, 0.35, 0.6 for the quadrotor, side-by-side, and tiltwing respectively; the tiltwing gear is retractable. The side-by-side rotor support (wing) is a faired structure that does not generate lift. The tiltwing wing has a two-dimensional lift curve slope of 5.7, maximum lift coefficient of 2.0, Oswald factor 0.8, and zero-lift angle of –4.0 deg. Faired rotor hubs and low-drag pylons are assumed. The quadrotor hub drag coefficient includes the rotor support arms (so the support arm D/q scales with rotor radius squared).

Table 8. Aircraft component drag.

component	reference area	drag coefficient
fuselage	wetted area	0.0045
wing		
side-by-side	wing area	0.05
tiltwing	wing area	0.0095
rotor hub		
quadrotor	rotor disk area	0.0045
side-by-side	rotor disk area	0.0015
tiltwing	spinner wetted area	0.04
rotor pylon		
quadrotor	wetted area	0.025
side-by-side	wetted area	0.015
tiltwing	wetted area	0.010

Aircraft and Rotor Models

The reference atmosphere (used with design C_W/σ and tip speed to calculate rotor solidity) is 5k/ISA+20°C.

The aircraft trim scheme obtains zero net force and moment on the aircraft by adjusting aircraft controls (collective, lateral cyclic, longitudinal cyclic, and pedal, connected to rotors and fixed wing controls as appropriate for the rotorcraft type) and aircraft attitude (pitch and roll angles). For symmetric aircraft, trim can use only the longitudinal loads and controls. For the tiltwing in conversion, wing flap is adjusted with the aircraft pitch angle fixed. For the turboelectric propulsion system, the generator power is adjusted in trim for zero battery energy flow, so generator power equals the required motor power.

Efficient rotor performance is obtained, and calculated using CAMRAD II, including distributed multi-rotor interactions (rotor-rotor, rotor-wing, rotor-airframe). The NDARC performance model is calibrated based on single and twin-rotor performance. Design C_W/σ is chosen considering advanced technology, and the maximum advance ratio in edgewise flight. The quadrotor and side-by-side aircraft use $C_W/\sigma = 0.10$, while the tiltwing uses $C_W/\sigma = 0.14$ (based on XC-142A). For low noise, the hover tip speed is much lower than conventional rotorcraft: 450 ft/sec for the quadrotor, 550 ft/sec for the side-by-side and tiltwing. For efficient cruise, the tiltwing operates at 50% hover tip speed. For best cruise performance, the side-by-side rotors rotate with outboard blades forward. For good wing stall characteristics (based on XC-142A), the tiltwing propellers rotate with outboard blades upward in cruise.

The rotor geometry, including twist, taper, and tip geometry was optimized for performance using CAMRAD II calculations for hover and cruise flight conditions.

The quadrotor hubs are at lateral and longitudinal stations ±1.35R (35% separation, arm length 1.91R). For rotor speed control, the fixed collective pitch value is based on the hover performance with collective control and design tip speed. Flapping (flap frequency 1.03/rev, 4% hinge offset) and hingeless (flap frequency 1.25/rev) rotors are considered. The three-bladed rotors use modern airfoils, $-12/-13$ deg twist (flapping or hingeless, respectively), 75% taper, with aircraft center-of-gravity 0.9/0.4 ft forward of the midpoint between the rotors for best cruise performance. The rear rotors are 0.35R above the front rotors. The flapping rotor has 45 deg of δ_3 (pitch-flap coupling), which reduces flapping relative the shaft by about a factor of 2 in cruise.

The rotors of the side-by-side aircraft are overlapped by 15% (span = 85% rotor diameter) for optimum cruise performance (ref. 9). The rotor support (wing) is a non-lifting, faired structure, with aspect ratio of 15 and thickness-to-chord ratio of 40%. The four-bladed flapping rotors (flap frequency 1.035/rev) have -12 deg of twist, modern airfoils, and swept-tapered tips (15 deg sweep and 60% taper from 94%R).

The tiltwing span is 4.2 times the propeller diameter, with a thickness-to-chord ratio of 18% (based on XC-142A). The inboard hub is 1.75R from the centerline (0.50R fuselage width, 0.25R clearance), the outboard hub is at 3.6R (1.85R between hubs, 7.5% overlap), and the wing tip is 0.6R from the outboard hub. Because of the low tip speed, the propellers have high solidity, with 10 blades, 75% taper, and inboard/outboard twist of $-40/-38$ deg. The propeller wake velocity is included in the calculation of the wing angle of attack.

The aircraft disk loading was optimized for performance (weight, power, energy) using NDARC, with resulting disk loadings typical of helicopters with the same gross weight.

CONCEPT VEHICLES

Quadrotor with Electric Propulsion

The single-passenger (250-lb payload), 50-nm range quadrotor with electric propulsion is shown in figures 1 and 6; figure 7 illustrates the propulsion system architecture. The passenger weight is higher than for the larger aircraft, since with only one passenger can not use mean weight. The four rotors are in the X-arrangement (pair of tandem rotors). For good performance, reduced vibration, and improved handling qualities, the rear rotors are above the front rotors and the center-of-gravity is forward of the mid-point between the rotors. The tip speed is 450 ft/sec (low noise), and the disk loading is 2.5 lb/ft^2 (optimum weight, power, energy). The baseline aircraft uses collective control (for control bandwidth and autorotation capability), flapping rotors (for low weight, loads, and vibration), and an interconnect shaft (for power distribution and control in OEI/AEI conditions).

Table 9 gives design details for the baseline aircraft, as well as for aircraft with rotor speed control, hingeless rotors, and turboshaft or reciprocating or diesel engines. Figure 8 shows the sensitivity of the electric aircraft weight to design mission range. Doubling the range to 100 nm increases the design gross weight by 50%. The NDARC design does not close at 200 nm range. With an internal combustion engine, the aircraft weight is much less sensitive to range. Doubling the range to 100 nm increases the design gross weight by 2% with a diesel engine, or by 6% with a turboshaft engine, with converged NDARC designs up to 1400 nm. For small range, the turboshaft engine gives the smallest aircraft weight (table 9), due to its small weight/power. For large range (not shown in table 9), the diesel-powered aircraft is smallest (60% of turboshaft aircraft weight for 600 nm range), due to its good specific fuel consumption. The electric and turboshaft quadrotor designs fly the mission at 70 knots, since V_{max} is below V_{br}. Flying the mission at higher speeds increases the aircraft weight and power. Converged NDARC designs can be obtained up to 100 knots with flapping rotors, up to 135 knots with hingeless rotors.

Side-by-Side with Turboshaft Hybrid Propulsion

The six-passenger (1200-lb payload), 200-nm range side-by-side aircraft with turboshaft hybrid propulsion is shown in figures 2 and 9; figure 10 illustrates the propulsion system architecture. The two rotors are side-by-side, with 15% overlap for cruise performance optimization. The tip speed is 550 ft/sec (low noise), and the disk loading is 4.5 lb/ft^2 (optimum weight, power, energy). The parallel hybrid propulsion system has two turboshaft engines, plus a motor/generator and battery. The 100 hp motor is used for hover and low speed flight, and in cruise the motor charges the battery. The battery is sized for 10 min (five 2-min segments) hover. The baseline aircraft uses an interconnect shaft (for power distribution and control in OEI/AEI conditions).

Table 10 gives design details for the baseline aircraft, as well as for aircraft with turboshaft or electric propulsion. The design range is 100 nm for electric propulsion. Figure 11 shows the sensitivity of the hybrid aircraft weight to design mission range. Doubling the range to 400 nm increases the design gross weight by 30%. The NDARC design does not close at 1800 nm range. Similar results are obtained for the aircraft with just turboshaft engines. For the electric aircraft, doubling the range to 200 nm increases the design gross weight by a factor of 2.2, and the NDARC design does not close at 220 nm range. These electric aircraft trends are similar for 1, 6, and 15 passenger designs. The side-by-side aircraft fly the mission at Vbr, which is about 110 knots (table 10). Flying the mission at higher speeds increases the aircraft weight and power. Converged NDARC designs can be obtained for mission speeds up to 170 knots.

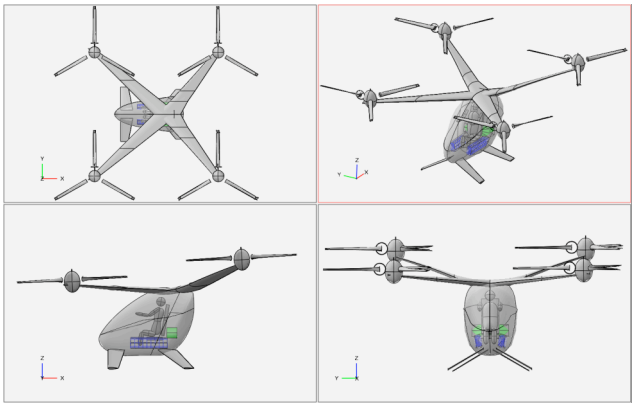

Figure 6. Single-passenger quadrotor with electric propulsion.

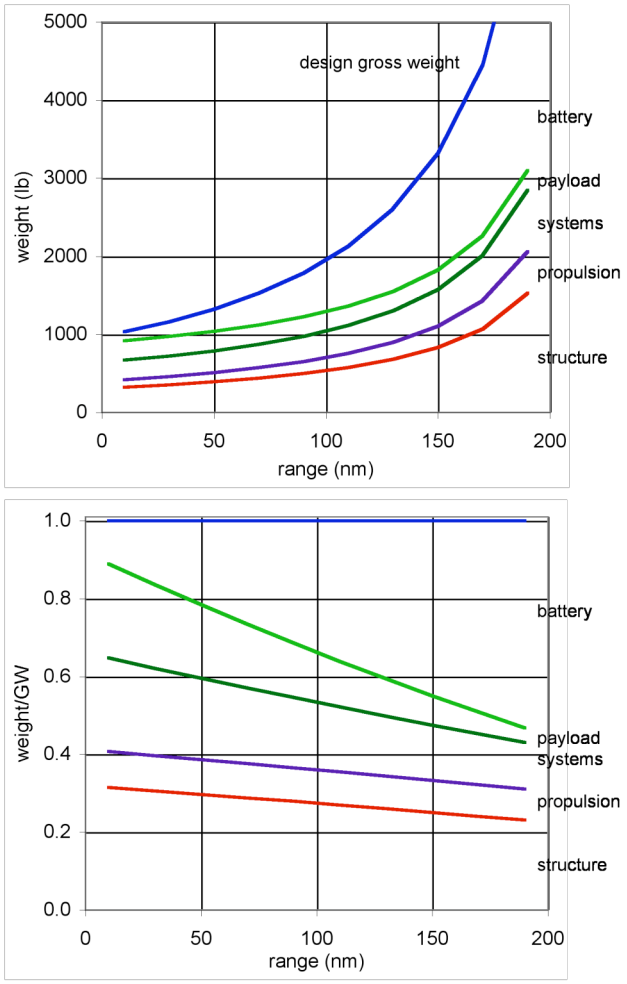

Figure 8. Electric quadrotor aircraft weight variation with design mission range (the right-hand-side labels identify the weight group between the lines).

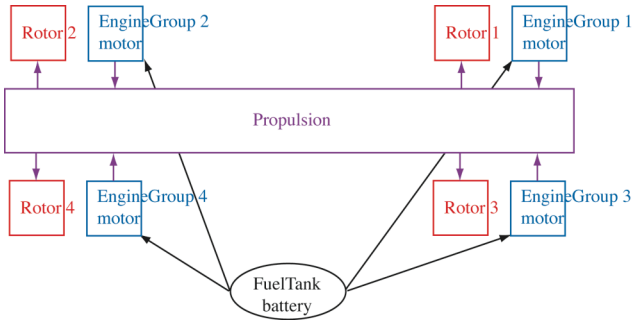

a) Electric, collective control

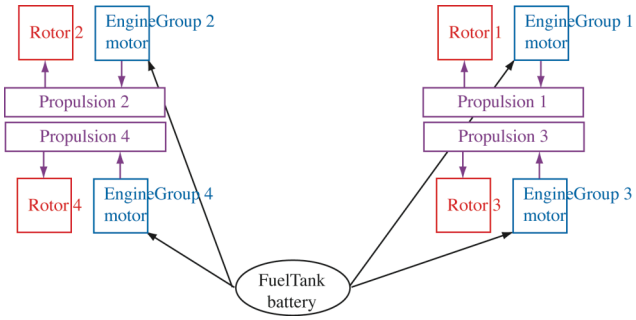

b) Electric, rotor speed control

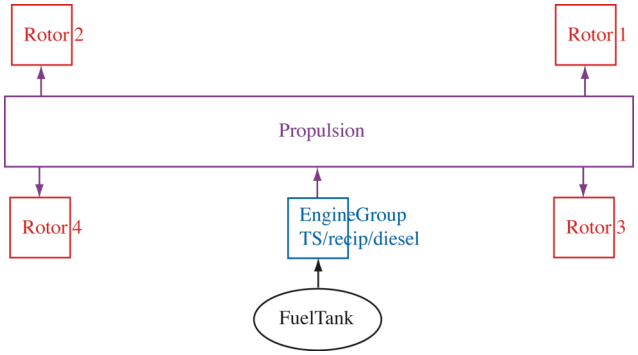

c) Turboshaft or reciprocating engine, collective control

Figure 7. Quadrotor propulsion system architecture.

Table 9. Quadrotor concept vehicle design.

	electric	rpm control	hingeless	turboshaft	recip	diesel
disk loading (lb/ft^2)	2.5	2.5	2.5	2.5	2.5	2.5
radius (ft)	6.31	6.22	6.94	5.65	6.06	5.96
solidity	0.0646	0.0646	0.0646	0.0646	0.0646	0.0646
autorotation index	1.63	1.50	2.78	1.16	1.27	1.49
power (hp)	4x21.6	4x22.5	4x25.7	93	100	83
sfc MCP SLS				0.869	0.476	0.380
weight/power	0.382	0.379	0.370	0.700	1.650	1.900
drag D/q (ft^2)	3.43	3.36	3.95	2.80	3.07	3.00
fuselage	0.58	0.58	0.58	0.58	0.58	0.58
rotor	2.65	2.58	3.17	2.02	2.30	2.22
D/q / (W/1000)$^{2/3}$	2.95	2.93	3.00	2.70	2.80	2.79
tank cap (MJ or lb)	178	168	214	51	30	20
battery or tank weight (lb)	272	257	327	20	16	13
DGW (lb)	1252	1217	1511	1001	1153	1116
WE (lb)	997	961	1256	695	868	841
structure	348	366	480	303	347	337
rotor group	137	133	241	111	127	123
fuselage group	108	131	123	95	102	100
propulsion	385	352	460	156	268	253
drive system	57	38	71	50	52	49
systems	185	166	190	180	184	183
flight controls	58	40	61	56	57	57
WO (lb)	1002	966	1261	700	873	846
V_{br} (knots)	86	83	86	99	92	84
V_{be} (knots)	50	48	48	49	50	50
V_{max} (knots)	71	66	69	86	94	102
payload (lb)	250	250	250	250	250	250
range (nm)	50	50	50	50	50	50
TO GW (lb)	1252	1216	1511	997	1152	1115
TO WO (lb)	1002	966	1261	700	873	846
TO fuel weight (lb)				48	29	20
TO fuel energy (MJ)	177	168	214			
fuel burn (MJ or lb)	130	124	157	35	21	15
cruise speed (knots)	70	70	70	70	92	84
aircraft L/D_e = WV/P	5.24	5.34	5.22	5.08	5.19	5.28
aircraft FM	0.71	0.71	0.72	0.70	0.70	0.70
V/V_{tip}	0.26	0.29	0.26	0.26	0.35	0.32
C_T/σ front	0.105	0.104	0.110	0.105	0.105	0.105
C_T/σ rear	0.095	0.104	0.090	0.094	0.095	0.095
total hover FM	0.77	0.77	0.77	0.77	0.77	0.77
total cruise L/D_e	7.55	7.82	7.25	7.56	8.96	8.59
hover current 1/hr	1.41	1.45	1.40			
cruise current 1/hr	0.89	0.90	0.90			
$W_{battery}$/GW	0.217	0.211	0.216			
WO/GW (without battery)	0.583	0.583	0.618	0.701	0.758	0.758
WO/GW	0.800	0.794	0.835	0.701	0.758	0.758
W_{fuel}/GW				0.048	0.025	0.018
$W_{payload}$/GW	0.200	0.206	0.165	0.251	0.217	0.224

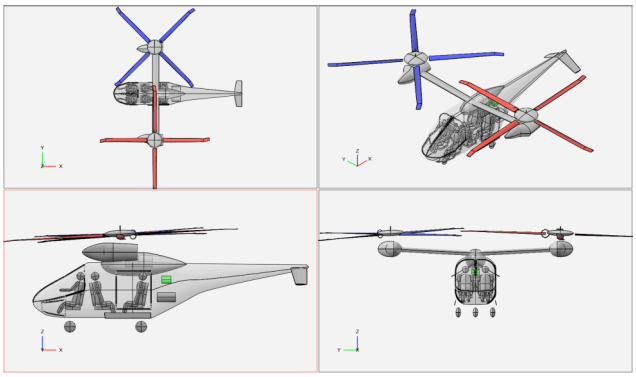

Figure 9. Six-passenger side-by-side helicopter with hybrid propulsion.

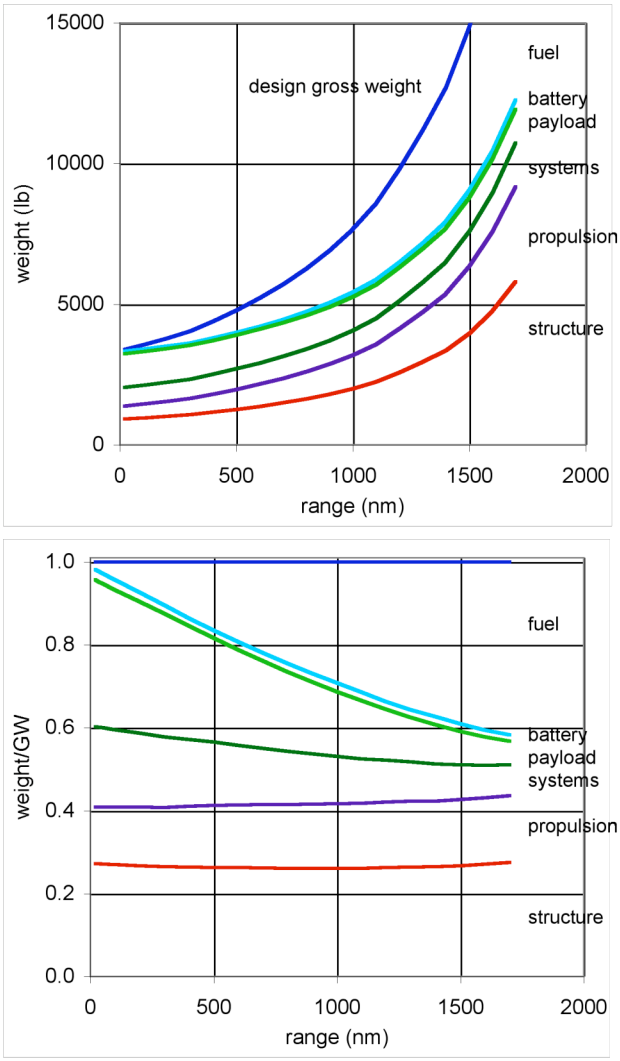

Figure 11. Hybrid side-by-side aircraft weight variation with design mission range (the right-hand-side labels identify the weight group between the lines).

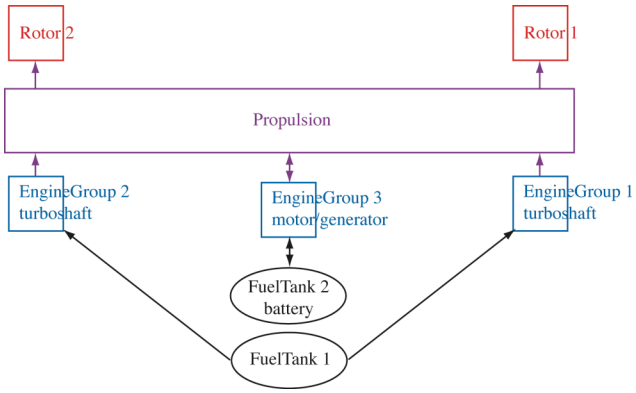

a) Turboshaft hybrid

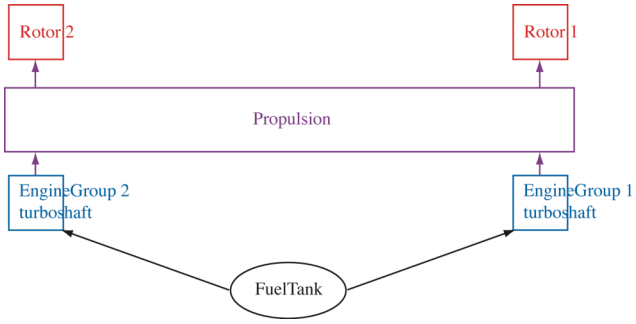

b) Turboshaft

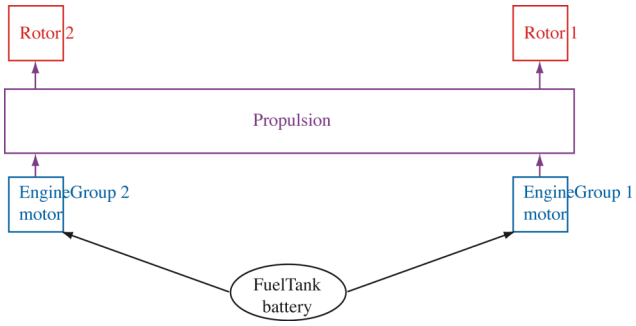

c) Electric

Figure 10. Side-by-side propulsion system architecture.

Table 10. Side-by-Side concept vehicle design.

	hybrid	turboshaft	electric		hybrid	turboshaft	electric
disk loading (lb/ft^2)	4.5	3.5	3.5	V_{br} (knots)	114	113	100
radius (ft)	11.82	13.26	15.94	V_{be} (knots)	65	60	62
solidity	0.0779	0.0606	0.0606	V_{max} (knots)	127	121	114
autorotation index	1.15	1.26	1.80	payload (lb)	1200	1200	1200
power (hp)	2x187	2x219	2x236	range (nm)	200	200	100
sfc MCP SLS	0.577	0.574		TO GW	3922	3831	5585
weight/power	0.500	0.500	0.236	TO WO	2400	2302	4385
motor/gen power	100			TO fuel weight (lb)	322	329	
weight/power	0.287			fuel burn (lb)	289	297	
drag D/q	5.92	6.67	8.22	TO battery energy (MJ)	66		1083
fuselage	1.59	1.59	1.59	battery energy burn (MJ)	60		902
rotor	2.35	2.67	3.31	cruise speed (knots)	115	113	100
wing	1.35	1.69	2.45	aircraft $L/D_e = WV/P$	5.98	6.21	7.32
$D/q / (W/1000)^{2/3}$	2.30	2.64	2.61	aircraft FM	0.69	0.67	0.69
tank cap (lb)	350	364		C_T/σ	0.105	0.104	0.105
battery cap (MJ)	66		1116	V/V_{tip}	0.35	0.35	0.31
fuel tank wt (lb)	67	69		rotor hover FM	0.82	0.81	0.81
battery wt (lb)	101		1708	rotor cruise L/D_e	11.39	12.53	12.17
DGW (lb)	3950	3866	5584	hover current 1/hr	4.77		1.21
WE (lb)	2390	2292	4375	cruise current 1/hr	0.25		0.64
structure	1050	1076	1404	Wbattery/GW	0.026	0.000	0.306
wing group	131	140	197	WO/GW (without battery)	0.586	0.601	0.479
rotor group	248	265	420	WO/GW	0.612	0.601	0.785
fuselage group	374	368	466	W_{fuel}/GW	0.082	0.086	0.000
propulsion	665	558	2144	$W_{payload}/GW$	0.306	0.313	0.215
drive system	218	214	289				
systems	508	497	520				
flight controls	98	87	102				
WO (lb)	2400	2302	4385				

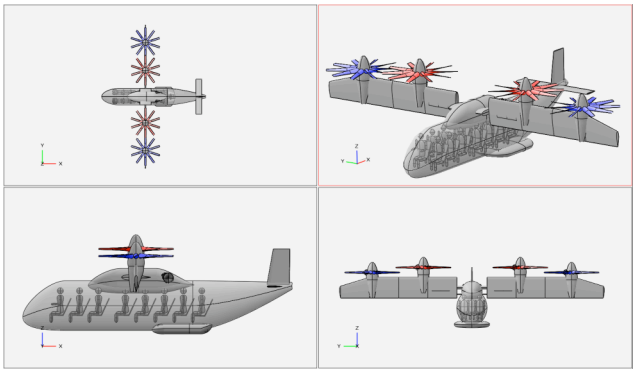

Figure 12. Fifteen-passenger tiltwing with turboelectric propulsion.

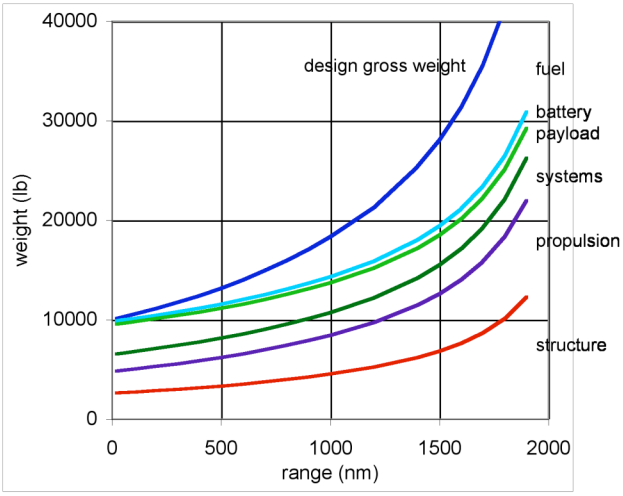

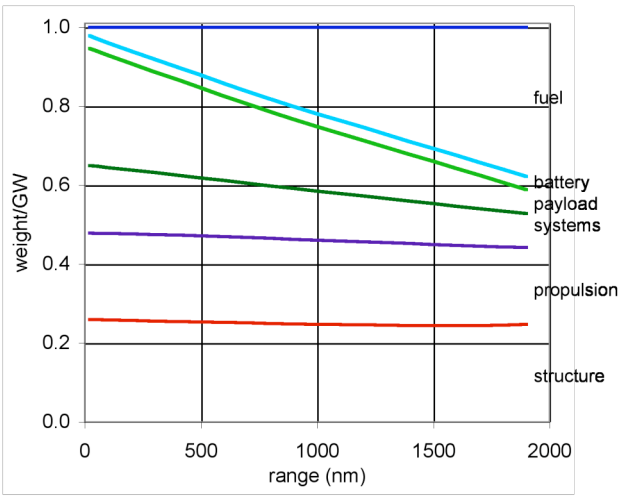

Figure 14. Turboelectric tiltwing aircraft weight variation with design mission range (the right-hand-side labels identify the weight group between the lines).

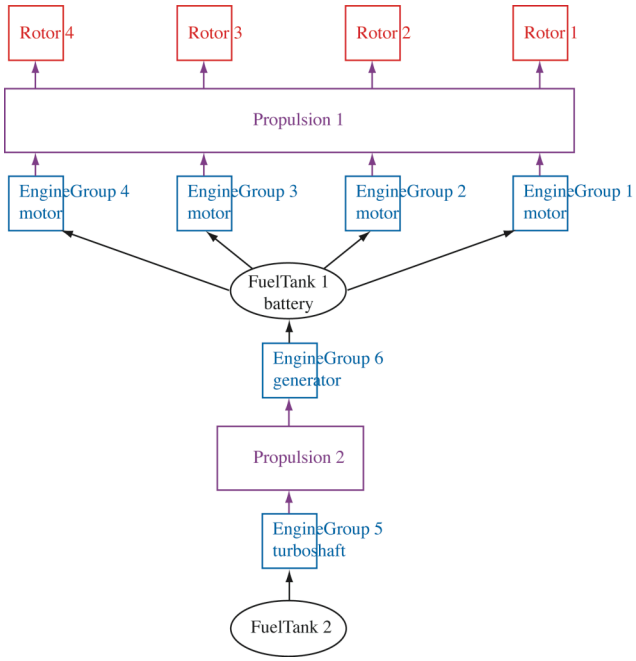

a) Turboelectric

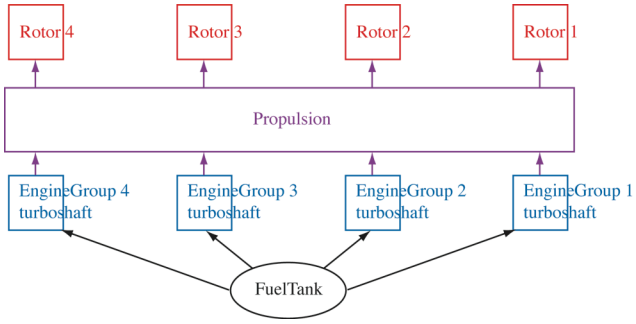

b) Turboshaft

Figure 13. Tiltwing propulsion system architecture.

Table 11. Tiltwing concept vehicle design.

	turboelectric	turboshaft	tailprop		turboelectric	turboshaft	tailprop
disk load (lb/ft^2)	30	30	30	DGW (lb)	14039	11856	14193
radius (ft)	6.10	5.61	6.14	WE (lb)	8918	6518	9068
solidity	0.3707	0.3707	0.3707	structure	3495	2973	3520
tail prop DL			20	wing group	822	686	831
radius (ft)			4.65	rotor group	503	431	502
solidity			0.2471	fuselage group	1129	1018	1137
wing load (lb/ft^2)	60	60	60	propulsion	3460	1810	3619
wing span (ft)	51.26	47.11	51.54	drive system	715	580	748
aspect ratio	11.23	11.23	11.23	systems	1338	1278	1294
power (hp)	4x731	4x862	4x731	flight controls	394	348	344
sfc MCP SLS		0.491		WO (lb)	8938	6538	9088
weight/power	0.198	0.230	0.198	V_{br} (knots)	200	184	192
turboshaft power	4730		4733	V_{be} (knots)	122	117	117
sfc MCP SLS	0.348		0.348	V_{max} (knots)	230	215	227
weight/power	0.132		0.132	payload (lb)	3000	3000	3000
generator power	3239		3242	range (nm)	400	400	400
weight/power	0.150		0.150	TO GW	13866	11654	14009
drag D/q (ft^2)	8.22	8.81	8.37	TO WO	8938	6538	9088
fuselage	2.58	2.58	2.58	TO fuel Wt (lb)	1928	2116	1921
rotor	2.18	3.39	2.29	fuel burn (lb)	1753	1923	1747
wing	2.22	1.88	2.25	cruise speed (knots)	200	183	192
D/q / (W/1000)$^{2/3}$	1.43	1.68	1.44	aircraft $L/D_e = WV/P$	7.22	7.28	7.70
battery cap (MJ)	288		288	aircraft FM	0.67	0.76	0.68
tank cap (lb)	2101	2318	2105	V/V_{tip}	1.23	1.12	1.18
battery wt (lb)	441		441	C_T/s	0.138	0.137	0.137
fuel tank wt (lb)	248	267	249	total hover FM	0.79	0.79	1.05
				total propulsive eff	0.82	0.85	0.82
				$W_{battery}/GW$	0.032	0.000	0.032
				WO/GW (wo battery)	0.613	0.561	0.617
				WO/GW	0.645	0.561	0.649
				W_{fuel}/GW	0.139	0.182	0.137
				$W_{payload}/GW$	0.216	0.257	0.214

Tiltwing with Turboelectric Propulsion

The fifteen-passenger (3000-lb payload), 400-nm range tiltwing aircraft with turboelectric propulsion is shown in figures 3 and 12; figure 13 illustrates the propulsion system architecture. The four propellers are on a tilting wing, arranged so the wing is completely immersed in the prop-wash. The tip speed is 550 ft/sec in hover (low noise) and 275 ft/sec in cruise (50%, for performance). The rotors have a disk loading of 30 lb/ft^2 (for conversion) and wing loading of 60 lb/ft^2 (for conversion and aspect ratio). The disk loading is high compared to helicopter rotors, but low compared to successful tiltwing aircraft. The combination of low tip speed and this disk loading results in high solidity of the propellers. Increasing the number of propellers would either increase the wing aspect ratio (with an impact on wing weight and whirl flutter stability) or increase the disk loading and hence blade solidity.

The baseline aircraft uses single-axis cyclic control on the propellers (for effective pitch and yaw trim and control in helicopter mode), and an interconnect shaft (for power distribution and control in OEI/AEI conditions). The turboelectric propulsion system has a single high-efficiency turboshaft engine driving a generator, which powers four electric motors. The battery is sized for 2-min hover in the event of the turboshaft or generator not functioning.

Table 11 gives design details for the baseline aircraft, as well as for aircraft with turboshaft propulsion or tail propeller for pitch control. Figure 14 shows the sensitivity of the turboelectric aircraft weight to design mission range. Doubling the range to 800 nm increases the design gross weight by 30%. The NDARC design does not close at 2000 nm range. Similar results are obtained for the aircraft with just turboshaft engines.

RESEARCH AREAS FOR AIR TAXI AIRCRAFT DEVELOPMENT

Figure 4 summarizes the technology areas in which research is neeeded for air taxi aircraft development. These requirements are supported by the design of the concept vehicles, including numerous design excursions.

PROPULSION EFFICIENCY

Battery

The most important factor in the feasibility of electrical propulsion systems is the requirement for light-weight, high-power batteries. The baseline designs assume an installed specific energy of 400 Wh/kg. Current state-of-the-art batteries have installed specific energy of 100–150 Wh/kg. For the quadrotor with electric propulsion, the design using SOA batteries closes only with reduced range and high gross weight (figure 15), and with 300 Wh/kg the aircraft is 20% heavier. Closed designs are obtained for the side-by-side and tiltwing using SOA batteries, but battery technology level has a significant impact (figures 16 and 17), even though the batteries are relatively small. The hybrid side-by-side aircraft is 2% heavier for 300 Wh/kg, 12% heavier with 150 Wh/kg. The turboelectric tiltwing aircraft is 3% heavier for 300 Wh/kg, 18% heavier with 150 Wh/kg. The weight and power variation with range and battery technology is shown in figure 18 for the electric quadrotor, and in figure 19 for an electric side-by-side aircraft. Aircraft size does not change the conclusions from these figures, as similar results are obtained for both single-passenger and fifteen-passenger side-by-side designs.

The power capability of batteries is also important. High power is obtained with high current, and current can be characterized by fraction x of the charge capacity C: $I = xC$, with units of 1/hr for x. A maximum burst discharge current of 10C to 30C (fully discharged in 6 to 2 minutes) is possible for emergency use, but long battery life typically requires currents of 1C to 3C. The discharge current variation with range is shown in figure 20 for the electric quadrotor, and in figure 21 for an electric side-by-side aircraft. The cruise current is less than the hover current for these designs, since cruise speed is fallout and the power is sized by the hover condition. The battery capacity is the sum of hover, cruise, and reserve requirements:

$$E_{\text{cap}=} = E_{\text{cruise}} + E_{\text{hover}} + E_{\text{reserve}}$$

Writing cruise power in terms of the aircraft effective lift-to-drag ratio ($P_c = WV/(L/D_e)$), the cruise energy is proportional to range:

$$E_{\text{cruise}} = (P_c/\eta_c) \times \text{time} = WV \times \text{time}/((L/D_e)\eta_c)$$
$$= WR/((L/D_e)\eta_c)$$

where η_c is the propulsion system efficiency in cruise, and $R = V \times \text{time}$ is the range. From the charge capacity $C_{\text{cap}} = E_{\text{cap}}/v$ (voltage v), and hover current $I = (P_h/v)/\eta_h$ (η_h is propulsion system efficiency in hover), the hover discharge current is

$$x_{\text{hover}} = I/C_{\text{cap}} = P_h/(\eta_h E_{\text{cap}})$$
$$= W\sqrt{W/2\rho A}/FM/(\eta_h E_{\text{cap}})$$

with hover power in terms of figure of merit ($P_h = W\sqrt{W/2\rho A}/FM$). Substituting for E_{cap} gives

$$1/x_{\text{hover}} = R\frac{\eta_h FM}{\eta_c (L/D_e)}/\sqrt{W/2\rho A} + \text{constant}$$

where the constant comes from the hover and reserve energy capacity. Ignoring the constant gives

$$x_{\text{hover}} = \sqrt{W/2\rho A}\ \frac{\eta_c (L/D_e)}{\eta_h FM}\ \frac{1}{R}$$

High hover efficiency (low disk loading and high figure of merit) reduces the current, but short range or high cruise efficiency (L/D_e) reduces the battery capacity required, hence increases the hover current x_{hover}. As illustrated in figures 20 and 21, this result is independent of battery technology, except as it impacts the range that is achievable by a design. For the quadrotor, the hover current $I_{\text{hover}} < 1C$ if the range is greater than 90 nm, $I_{\text{hover}} < 2C$ if the range is greater than 30 nm. There is some impact of size: for the side-by-side aircraft, the hover current $I_{\text{hover}} < 1C$ if the range is greater than 140/150/170 nm, $I_{\text{hover}} < 2C$ if the range is greater than 50/60/70 nm, for 1/6/15-passenger designs respectively.

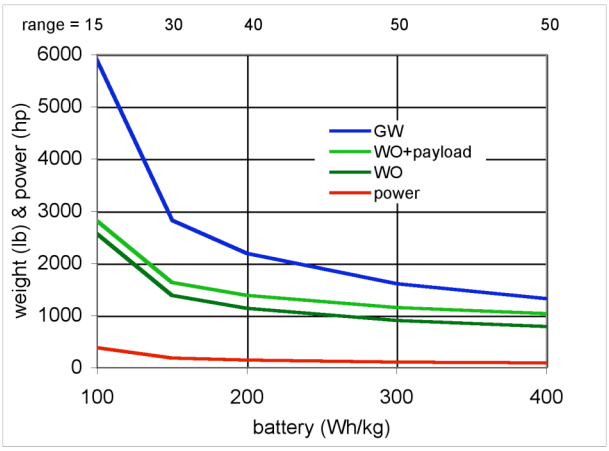

Figure 15. Electric quadrotor weight and power variation with battery installed specific energy.

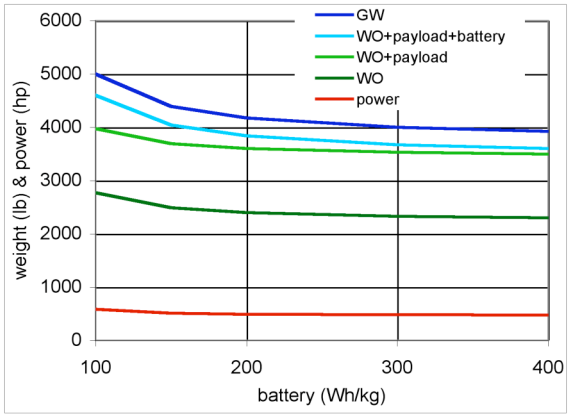

Figure 16. Hybrid side-by-side weight and power variation with battery installed specific energy.

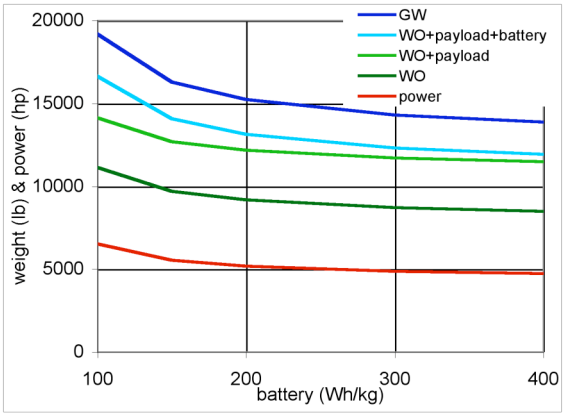

Figure 17. Turboelectric tiltwing weight and power variation with battery installed specific energy.

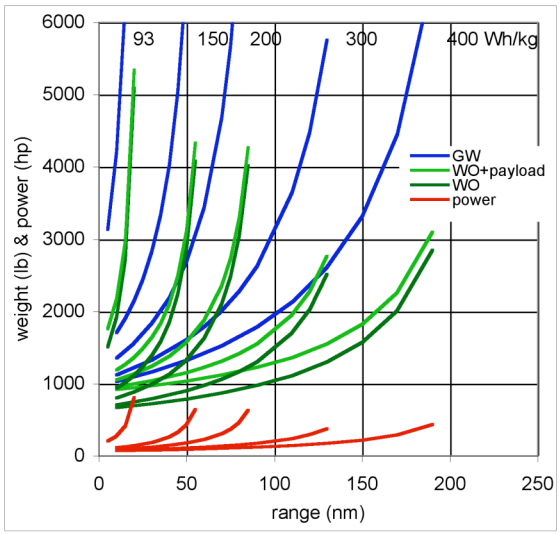

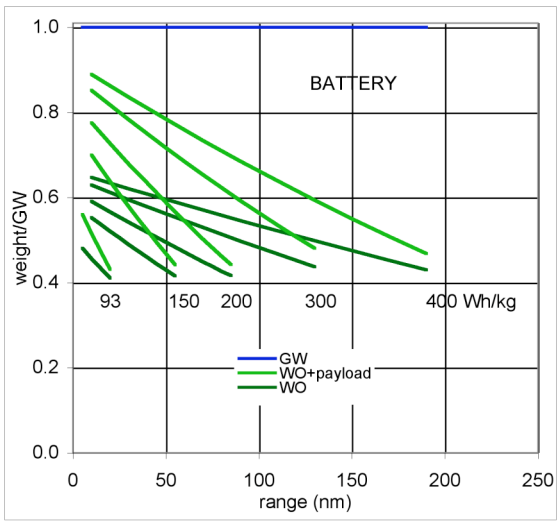

Figure 18. Electric quadrotor weight and power variation with range and battery technology.

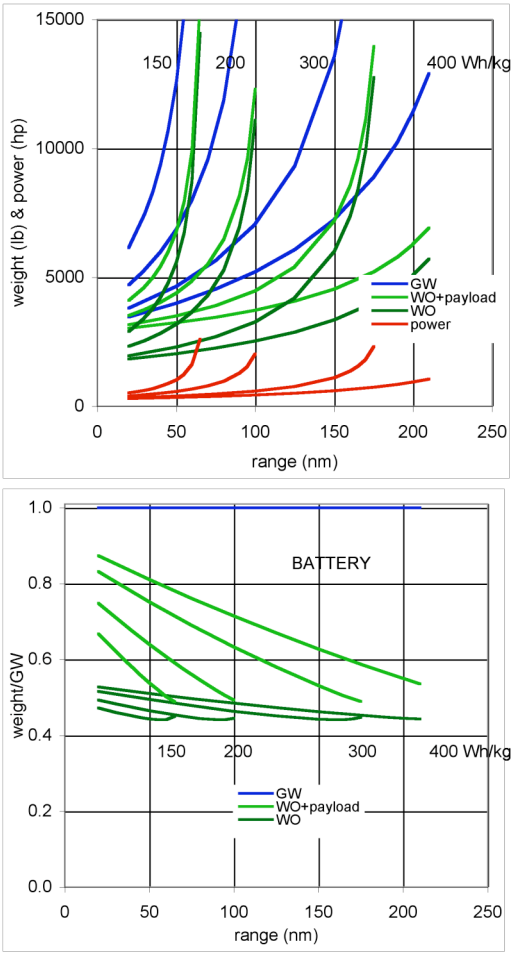

Figure 19. Electric side-by-side weight and power variation with range and battery technology.

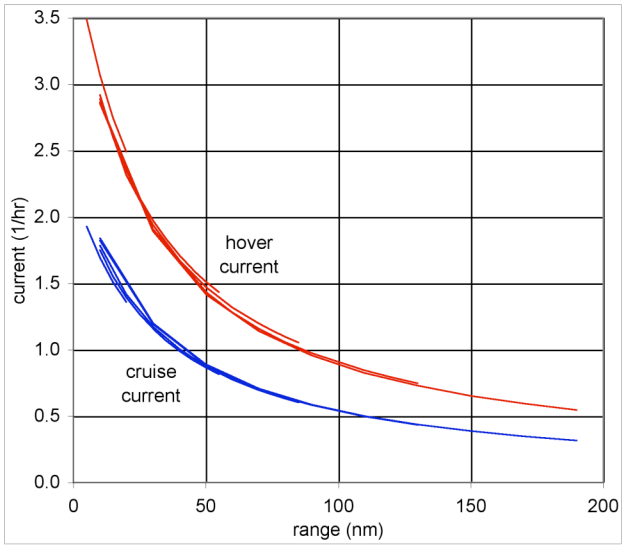

Figure 20. Electric quadrotor discharge current variation with range, for battery technology 93 to400 Wh/kg.

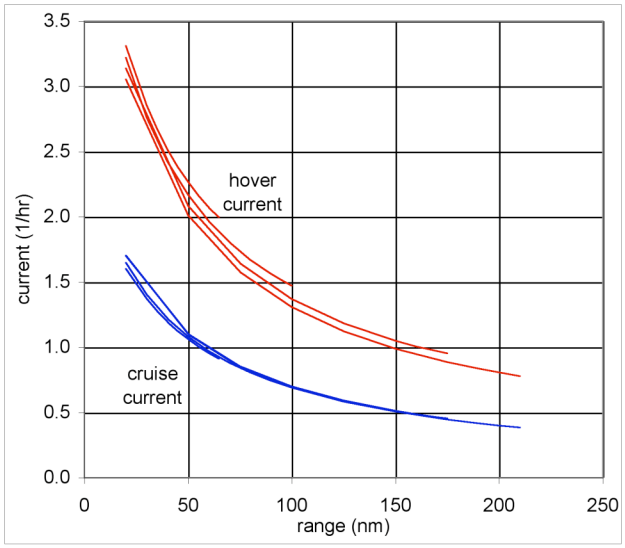

Figure 21. Electric side-by-side discharge current variation with range, for battery technology 150 to 400 Wh/kg.

Motors, Engines, and Drives

Light, efficient, high-speed electric motors are needed for these concept vehicles. Electric motors can have good weight efficiency, but power electronics and thermal management add significantly to the system weight. Hybrid propulsion systems need light, efficient internal combustion engines, either low weight/power diesels or low specific fuel consumption for small turboshafts. Mechanical gears remain the best way to transfer power, and to convert from low-torque motive power to high-torque rotors, so efficient drives are an important aspect of the designs.

PERFORMANCE

The use of electrical propulsion will be enabled by aerodynamic efficiency of the aircraft, so optimization of the performance is important. The aircraft, rotor/propeller, and blade geometry can be optimized using a comprehensive analysis, with emphasis on critical hover and cruise flight conditions for aircraft sizing.

Aircraft Optimization

Disk loading is chosen to minimize aircraft weight, power, and energy. For small aircraft with edgewise moving rotors, low disk loading reduces hover power. The optimum is 2.5 lb/ft^2 for the single-passenger quadrotor, and 4.5 lb/ft^2 for the six-passenger side-by-side. Tiltwing aircraft have been designed with high disk loading propellers, in order to use the prop-wash over the

wing to control separation on the wing during conversion. Here the tiltwing was designed with a disk loading of 30 lb/ft^2 and a wing loading of 60 lb/ft^2 (the ratio of disk loading and wing loading determines wing aspect ratio and wing-chord-to-rotor-diameter ratio). Disk loading of 30 lb/ft^2 is high for a rotorcraft, implying high hover power and downwash, but for good conversion characteristics, successful tiltwing aircraft used disk loadings of 35–55 lb/ft^2, and with DL/WL=0.75. Figure 22 shows the weight and power of the tiltwing as a function of propeller disk loading. Minimum aircraft weight (10% below baseline) is at a disk loading of 12 lb/ft^2, but disk loading below 9 gives best power, fuel burn, and aircraft L/D. Since speed is fallout, as the disk loading is reduced from 30 to 9 lb/ft^2 the maximum speed is reduced from 226 to 154 knots (V_{br} is about 88% of V_{max}).

The rotors of the side-by-side aircraft are overlapped by 15% (span = 85% rotor diameter) for optimum cruise performance (ref. 9). Relative to a single main rotor (with same blade area) or non-overlapped side-by-side rotors, this geometry typically reduces the gross weight by 12%, power by 41%, and fuel burn by 35%.

The 30 lb/ft^2 disk loading and low tip speed of the tiltwing propellers leads to a large solidity ratio (σ = 0.37). Cruise performance is significantly improved by reducing the tip speed further. Table 12 shows the improvement possible in both hover and cruise performance using 50% rather than 75% tip speed reduction. Since a large number of blades is used to obtain the required solidity, a stacked propeller design (two co-rotating 5-bladed propellers) should be considered, which would require optimizing blade axial separation and azimuthal phase.

For the quadrotor, both collective and rotor speed control are considered. Figure 23 shows the trim operating conditions of the front and rear rotors for the two control methods. The longitudinal center-of-gravity position was set to minimize the cruise power, by producing closer front and rear rotor thrusts at the cruise flight speed.

Rotor Shape Optimization

The blade planform and twist, including taper, sweep, and droop of the tip are optimized using the comprehensive analysis. Generally balancing hover and cruise performance is necessary, with system metrics (weight, power, energy) determining the best geometry.

Hub, Rotor Support, and Airframe Drag Minimization

Minimizing the aircraft total drag is important for efficient cruise and low energy requirements. Table 13 summarizes the drag of the concept vehicles. Faired hubs are assumed for the quadrotor and side-by-side. The rotor support drag in particular is an opportunity for drag reduction. The tiltwing in airplane mode is a very clean design, comparable to fixed-wing turboprop aircraft.

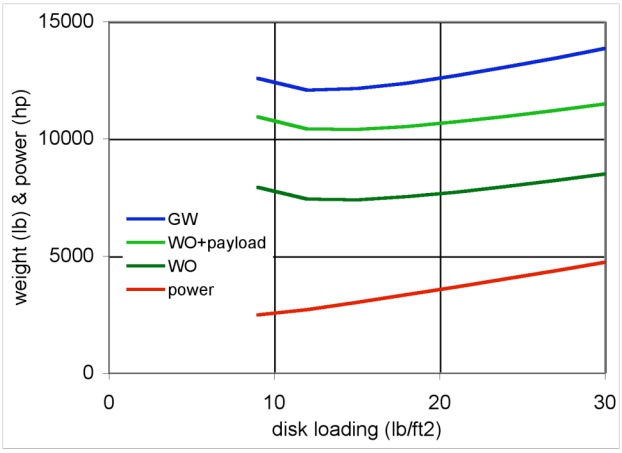

Figure 22. Turboelectric tiltwing weight and power variation with design disk loading.

Table 12. Tiltwing propeller performance optimization

cruise tip speed	75% hover	50% hover
C_T/σ hover	0.14	0.14
C_T/σ cruise	0.02	0.05
V/V_{tip} at V_{br}	0.66	1.00
twist	–56/–24	–40/–38
hover FM	0.75	0.81
cruise propulsive eff	0.74	0.85

Table 13. Aircraft drag D/q (ft^2)

	quadrotor		side-by-side		tiltwing	
total	3.43	100%	5.92	100%	8.22	100%
fuselage	0.58	17%	1.59	27%	2.58	31%
rotor	0.88	26%	2.35	40%	2.18	27%
rotor support	1.77	52%	1.35	23%		
wing					2.22	27%
other	0.20	5%	0.70	10%	1.24	15%
D/q / $(W/1000)^{2/3}$	2.95		2.30		1.43	

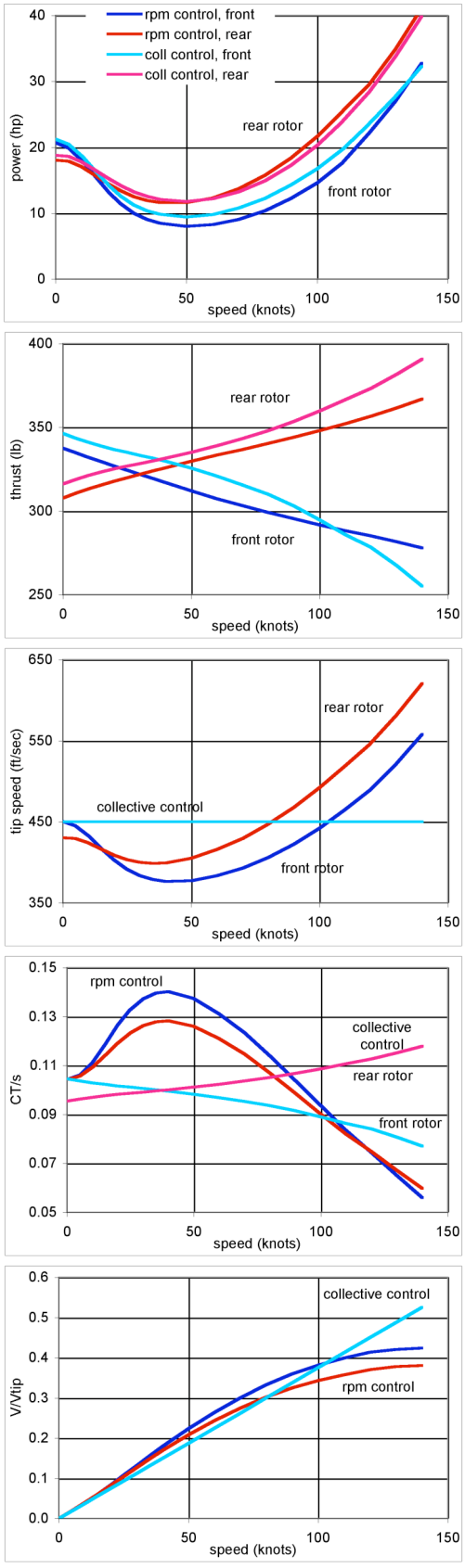

Figure 23. Electric quadrotor trim as a function of flight speed, for collective control and rotor speed control.

ROTOR-ROTOR INTERACTIONS

For aircraft with two or more main rotors, interactions between the rotors have a significant impact on performance, vibration, noise, and handling qualities. The interactions depend on the arrangement of the rotors. Figure 24 illustrates the wake geometry of the quadrotor and side-by-side aircraft in cruise flight. The overlap of the side-by-side rotors significantly improves the efficiency of cruise flight.

Elevating the rear rotors above the front rotors on the quadrotor reduces the cruise power, as shown in figure 25. Elevating the rear rotors is expected to reduce vibration and noise and improve handling qualities as well. Moving the aircraft center of gravity forward of the mid-point between the rotors, so the front and rear rotors trim closer to the same CT/s at cruise speed, further reduces the power (figure 25).

The effects of the rotor-rotor interactions may require vibration and load alleviation systems. The present designs have a weight allocation for vibration control.

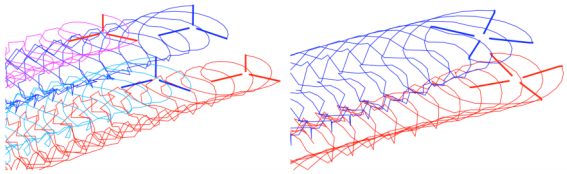

Figure 24. Wake geometry of quadrotor and side-by-side aircraft at cruise speed.

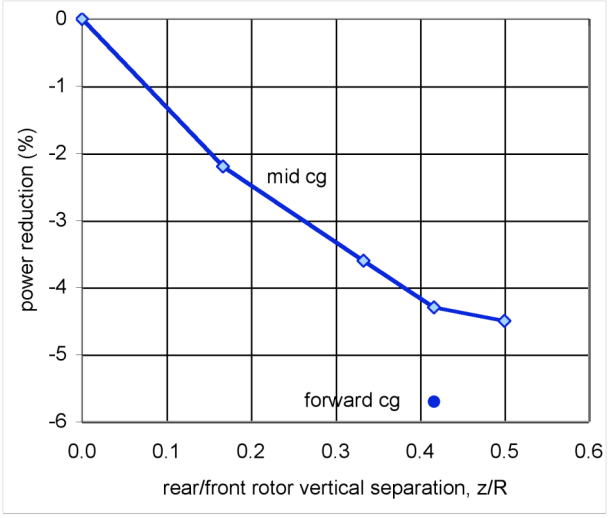

Figure 25. Influence of elevation of rear rotors on cruise performance of quadrotor.

ROTOR-WING INTERACTIONS

Rotor-wing interactions, and more generally aerodynamic interations, can impact performance and operation of the aircraft. Examples of known issues are hover download for tiltrotors, and wing separation or buffet during conversion for tiltwing aircraft. The tiltwing concept vehicle has been designed with a moderate disk loading (30 lb/ft^2) and wing loading (60 lb/ft^2). The NDARC analysis confirms that the design has sufficient power for level flight conversion from helicopter mode to airplane mode. The NDARC analysis also suggests that the wing is operating near or just beyond stall during conversion, but higher-fidelity aerodynamic analysis (comprehensive analysis or computational fluid dynamics) is required to investigate tiltwing conversion behavior. Increasing the disk loading would increase the propeller solidity and increase the downwash. Decreasing the disk loading would increase stall and buffet during conversion. Increasing wing loading would increase the wing aspect ratio, reducing the structural efficiency of the design.

Active flow control on the wing may be needed with the disk loading of the concept vehicle. An innovative structural design is needed for the high-aspect ratio wing, for light weight given the requirement for whirl flutter stability.

NOISE AND ANNOYANCE

All of the concept vehicles have been designed with low hover tip speed (450 ft/sec for the quadrotor, 550 ft/sec for the other aircraft), in anticipation of a significant requirement for noise reduction in the urban environment. Rotor-rotor interactions, such as rear rotors operating in the wake of front rotors, and wake interactions on retreating sides of overlapped side-by-side rotors, will increase blade-vortex interaction noise. Blade shape and spacing can be optimized for low blade-vortex-interaction and high-speed-impulsive noise.

Noise metrics and requirements are established by regulation for rotorcraft, but suitability and applicability of these to air taxi operations must to be established. Possibly new metrics will be required, and the new requirements may not be met by simply using low tip-speed rotors. Active control of rotor noise can achieve significant noise reductions, with 6 to 12 dB reduction demonstrated through analysis, wind tunnel test, and flight test of rotors (ref. 10).

AIRCRAFT DESIGN

Rotor or propeller design can have a significant impact on weight, vibration, and handling qualities. The electric quadrotor has flapping rotors (4% hinge offset), with 45 deg of δ_3 (pitch-flap coupling) to minimize flapping relative the shaft in forward flight, gusts, and maneuvers. With hingeless rotors, the rotor weight increase (due to higher blade and hub loads) results in about 25% larger design gross weight, with corresponding increases in power and energy. The vibration increase with hingeless rotors has been accounted for in the vibration control weight allocation, using 5%WE for hingeless rotors and 3%WE for flapping rotors. Active control of vibration may also be required, regardless of the hub type. Analysis, wind tunnel test, and flight test have demonstrated up to 90% reduction in loads and vibration using higher-harmonic control or individual-blade control (ref. 10). The rotor hub design, particularly flap frequency, also impacts the aircraft handling qualities.

STRUCTURE AND AEROELASTICITY

All of the concept vehicles require structurally efficient wing and rotor supports, stable coupled rotor and airframe dynamics, impact resistant structures, and crashworthy designs. Considering the innovations in aircraft type and propulsion system, and the requirements for air taxi operations, new design solutions and their impact on weight must be examined.

OPERATIONAL EFFECTIVENESS

Control

Air taxi operations are expected to require flight control systems with good disturbance rejection, which may impose constraints on control bandwidth and choice of control approach. Rotor control alternatives considered for the quadrotor are collective control, which can have the bandwidth needed as well as enabling autorotation of the aircraft; and rotor speed control, which must also have high bandwidth and requires a design solution for the all-motors-inoperative occurrence. Agility and disturbance rejection could also be improved on the quadrotor by using cyclic pitch control.

Control alternatives considered for the tiltwing are cyclic control (single axis) on the propellers; or tail propellers for pitch trim and control and for yaw control. Using just one tail propeller (for pitch control) increases the aircraft weight by 250 lb (1.1%). Consideration of failure modes would impact the design choice.

Air taxi operations will ultimately require all-weather capability, which is accounted for in the concept designs by the systems weight allocations.

Cost

Purchase cost of aircraft is roughly (20% accuracy) driven by aircraft empty weight, installed power, and complexity, plus the costs of electronic systems. For electric propulsion, the cost of batteries should be explicitly included in the purchase cost estimate.

Data is available for maintenance cost of helicopters flying traditional missions, but not for unconventional aircraft types engaged in air taxi operations.

A significant component of operating costs is the cost of fuel or energy. Figures 26 to 28 show this cost for the concept vehicles flying their design missions, with various propulsion systems. The vertical jumpts are the hover segments. Costs were calculated using November 2017 average US prices: $4.31/gal for jet A, $4.83/gal for aviation gasoline, $2.79/gal for diesel, $0.1098/kWh for electricity. We decline to speculate about future prices. For the quadrotor, energy cost for electrical propulsion is less than for diesel propulsion, and much lower than with a turboshaft (due to high specific fuel consumption). For the side-by-side aircraft, cost with electric propulsion is lower than with hybrid propulsion, although for half the design range. For the tiltwing, turboelectric costs are lower than turboshaft costs, due to lower specific fuel consumption.

SAFETY and AIRWORTHINESS

Airworthiness approval means a document, issued by the FAA for an aircraft, which certifies that the aircraft conforms to its approved design and is in a condition for safe operation (14 CFR 21.1(b)(2)). While certification requirements and procedures for air taxi aircraft may be debated, negotiated, or even contested, for aeromechanics research the focus is on safe operation. Every innovative aircraft type and non-traditional propulsion system requires an extensive failure mode, effects, and criticality analysis (FMECA). Important for air taxi aircraft are crashworthiness and the consequences of propulsion system failure. Crashworthiness requirements affect design of airframe structure, landing gear, and passenger accommodation and restraint. Propulsion system failures must be considered in detail. In particular, single as well as complete engine failure must be considered, with requirements for control and approaches for safe landing.

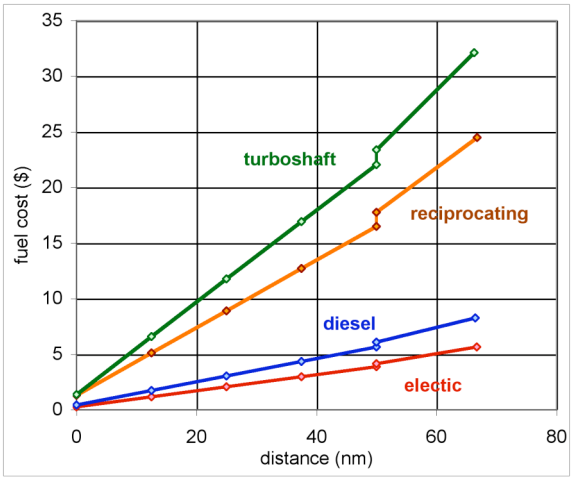

Figure 26. Quadrotor fuel or energy cost variation with distance for design mission.

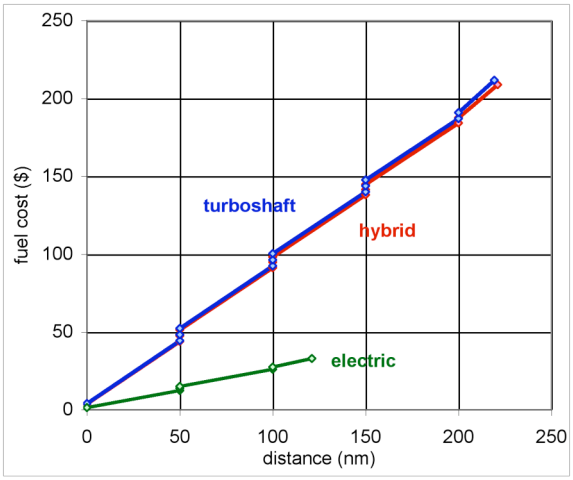

Figure 27. Side-by-side fuel or energy cost variation with distance for design mission.

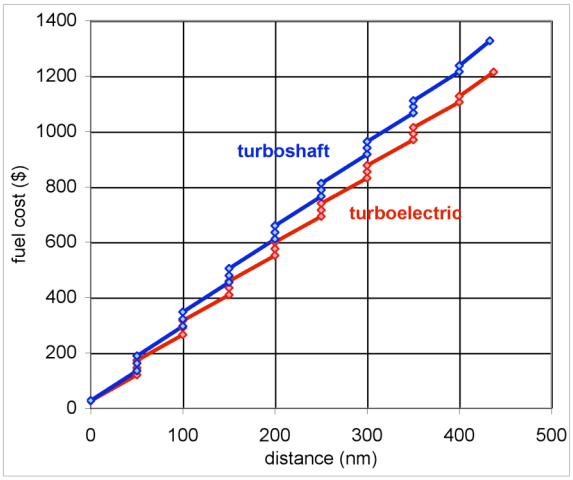

Figure 28. Tiltwing fuel or energy cost variation with distance for design mission.

Specific OEI/OMI operational scenarios and power requirements were not formulated for the design of these concept vehicles. Implications of a single motor or engine power failure can be assessed from figures 29 to 31, which show the power required and power available variation with speed, at design gross weight and 5k/ISA+20°C conditions. All engine operative power available is IRP at hover and low speed, MCP at cruise speeds. One engine inoperative power available is CRP. Level flight of the electric quadrotor OMI is possible for speeds greater than 20 knots (figure 29). Level flight of the hybrid side-by-side aircraft OEI or OMI is possible above 20 knots (figure 30); turboshaft propulsion is similar; electric propulsion OMI is possible above 30 knots. Level flight of the turboelectric (or turboshaft) tiltwing OMI is possible for speeds greater than 25 knots.

The electric quadrotor has collective control, and an interconnect shaft to maintain control and distribute power for one-motor-inoperative. For AEI, autorotation is enabled by low disk loading, collective control, and automatic failure recognition and control of entry and flair. An alternative design approach is to use rotor speed control, perhaps with more rotors and more motors on the aircraft, and with some design solution for all-motors-inoperative. The hybrid side-by-side aircraft has two engines and one motor to be considered for OEI; and low disk loading enables autorotation AEI. The turboelectric tiltwing has four engines with an interconnect shaft for OMI flight and control, and a battery sized for landing after failure of the turboshaft engine or generator.

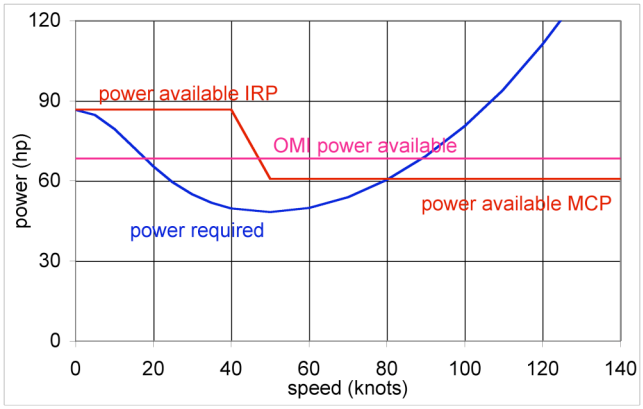

Figure 29. Electric quadrotor power required and power available variation with flight speed.

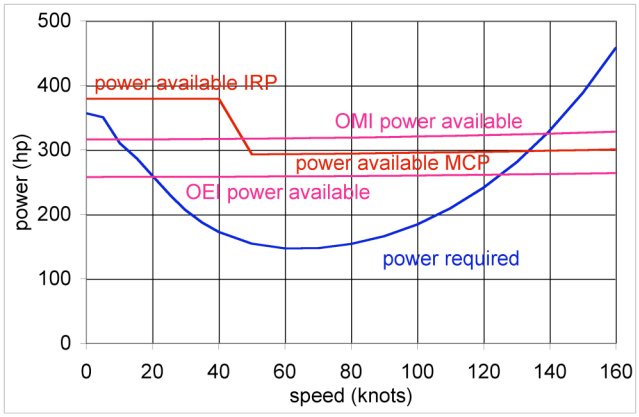

Figure 30. Hybrid side-by-side power required and power available variation with flight speed.

CONCLUDING REMARKS

Concept vehicles for air taxi operations have been described. Considering the design-space dimensions of payload (passengers and pilot), range, aircraft type, and propulsion system, three aircraft have been designed: a single-passenger (250-lb payload), 50-nm range quadrotor with electric propulsion; a six-passenger (1200-lb payload), 4x50 = 200-nm range side-by-side helicopter with hybrid propulsion; and a fifteen-passenger (3000-lb payload), 8x50 = 400-nm range tiltwing with turbo-electric propulsion. Based on the design of the concept vehicles, including numerous excursions, the research areas for air taxi aircraft development were discussed. These concept vehicles are expected to focus and guide NASA research activities in support of aircraft development for emerging aviation markets, in particular VTOL air taxi operations.

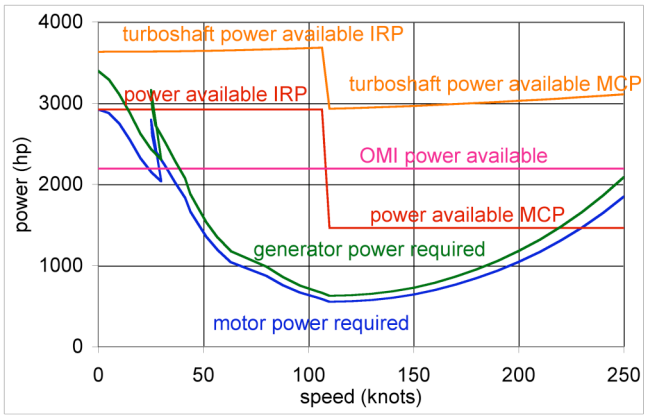

Figure 31. Turboelectric tiltwing power required and power available variation with flight speed.

Generally the tools available for rotorcraft aeromechanics analysis and design are applicable to VTOL air taxi aircraft, including comprehensive analyses, computational fluid dynamics codes, rotor and airframe structural analyses, and acoustic codes. However, component design methods and data bases are needed for unconventional aircraft propulsion systems, particularly the electrical subsystems, in order to have confidence in the results from NDARC.

The reliability of these tools in the design process rests on correlation of results with measured data for relevant aircraft types, systems, and components. Data from tests on the ground, in the wind tunnel, and in flight are needed to substantiate the aeromechanics analysis capability for air taxi aircraft. Correlation with such new test data will likely identify some requirements for development of improved or new analysis methods.

To meet the objectives of the paper, the concept vehicle designs were carried far enough to identify crucial technologies and research requirements. Refining these and similar designs requires more work on requirements definition, component performance and weight estimation, and exploration of aeromechanics behavior. Requirements need to be refined, including missions and propulsion system failure cases. Further optimization can be performed for the aircraft arrangement, including rotor locations and blade geometry. Better estimates are needed for propulsion components, including advanced technology battery and motor characteristics, motor controllers and thermal management weights, and advanced technology turboshaft and diesel engines. Refined estimates are needed for all weights, including fuselage and landing gear crashworthiness, drag of all components, and propulsion system losses (usually very optimistic). Tiltwing aerodynamic behavior in conversion must be analyzed, including correlation with flight test. Low-drag, light-weight rotor support structures should be designed and tested. For aircraft noise, metrics must be identified, requirements established, and the acoustic signatures of the concept vehicles assessed.

REFERENCES

1) Swartz, K.I. "Charging Forward. New eVTOL Concepts Advance." Vertiflite, 63:4 (July/August 2017).

2) Johnson, W. "NDARC. NASA Design and Analysis of Rotorcraft." NASA TP 2015-218751, April 2015.

3) Johnson, W. "NDARC — NASA Design and Analysis of Rotorcraft. Theoretical Basis and Architecture." American Helicopter Society Specialists' Conference on Aeromechanics, San Francisco, CA, January 2010.

4) Johnson, W. "NDARC — NASA Design and Analysis of Rotorcraft. Validation and Demonstration." American Helicopter Society Specialists' Conference on Aeromechanics, San Francisco, CA, January 2010.

5) Johnson, W. "Propulsion System Models for Rotorcraft Conceptual Design." American Helicopter Society 5th Decennial Aeromechanics Specialists' Conference, San Francisco, CA, January 2014.

6) Johnson, W., "Technology Drivers in the Development of CAMRAD II," American Helicopter Society Aeromechanics Specialist Meeting, San Francisco, California, January 1994.

7) Johnson, W. "Rotorcraft Aeromechanics Applications of a Comprehensive Analysis." HeliJapan 1998: AHS International Meeting on Rotorcraft Technology and Disaster Relief, Gifu, Japan, April 1998.

8) Johnson, W. "Rotorcraft Aerodynamic Models for a Comprehensive Analysis." American Helicopter Society 54th Annual Forum, Washington, D.C., May 1998.

9) Silva, C.; Johnson, W.; and Solis, E. "Multidisciplinary Conceptual Design for Reduced-Emission Rotorcraft." AHS Technical Conference on Aeromechanics Design for Transformative Vertical Flight, San Francisco, CA, January 2018.

10) Johnson, W. *Rotorcraft Aeromechanics*. New York: Cambridge University Press, 2013 (section 18.5.6).

NOMENCLATURE

AEI	all-engines inoperative
CRP	contingency rated power (typically 2.5 min)
DGW	design gross weight
IRP	intermediate rated power (typically 30 min)
ISA	international standard atmosphere
MCP	maximum continuous power
MRP	maximum rated power (typically 10 min)
OEI	one-engine inoperative
OGE	out-of-ground-effect
OMI	one-motor inoperative
sfc	specific fuel consumption
SLS	sea-level standard
SOA	state-of-the-art
TO	take off
VTOL	vertical take-off and landing

A	rotor disk area, πR^2
A_{blade}	total blade area
C	charge capacity (Wh or MJ)
C_T	rotor thrust coefficient, $T/\rho A V_{tip}^2$
C_W	aircraft weight coefficient, $W/\rho A V_{tip}^2$
D/q	drag divided by dynamic pressure
DL	disk loading, GW divided by total rotor disk area
FM	aircraft or rotor figure of merit
GW	gross weight (WO+payload+fuel)
I	current, I = xC
L	rotor lift
L/D_e	aircraft effective lift-to-drag ratio, WV/P
L/D_e	rotor effective lift-to-drag ratio, $LV/(P_o+P_i)$
P	power
P_o	profile power
P_i	induced power
R	rotor blade radius
T	rotor thrust
V	speed
V_{be}	best endurance speed (maximum 1/fuelflow)
V_{br}	best range speed (99% high side maximum V/fuelflow
V_{cruise}	cruise speed
V_{max}	maximum speed (power required = 90% MCP)
V_{tip}	rotor tip speed
W	weight
WE	aircraft empty weight
WL	wing loading, GW divided by wing area
WO	aircraft operating weight (WE+fixed useful load)
x	current (capacity per hour)
ρ	air density
σ	rotor solidity, A_{blade}/A